Environmental Pollution 363 (2024) 125244

Contents lists available at ScienceDirect

Environmental Pollution

journal homepage: www.elsevier.com/locate/envpol

Transforming urban air quality: Green infrastructure strategies for the urban centers of Ethiopia☆

Tikabo Gebreyesus [a,*], Christian Borgemeister [a], Cristina Herrero- Jáuregui [b], Girma Kelboro [a]

[a] Center for Development Research (ZEF), University of Bonn, Genscherallee 3, 53113 Bonn, Germany
[b] Departamento de Biodiversidad, Ecología y Evolución, Universidad Complutense de Madrid, 28040 Madrid, Spain

A R T I C L E I N F O

Keywords:
Urban green infrastructure
Air pollution removal
Economic values
BVOC emission
i-Tree Eco Model
Urban areas

A B S T R A C T

Urban green infrastructure (GI) plays a crucial role in improving air quality by removing pollutants and reducing emissions from structures. However, in Ethiopia, inadequate GI planning, largely due to limited awareness among planners and policymakers, can undermine the benefits of GI and worsen urban air quality issues. In this study, we demonstrate how the GI strategy approach can enhance air quality and assess the negative impacts of biogenic volatile organic compounds (BVOCs) emitted by certain tree species in Ethiopia, using Hawassa as a case study. We utilized a customized i-Tree Eco model to estimate annual pollutant removal and BVOC emissions and applied the Kriging method in ArcGIS to map their spatial distribution. In Hawassa, GI systems removed 274.2 t of pollutants annually, valued at \$1.79 million, with SO_2 being the most and CO the least removed pollutants. Air pollution removal was highest during the dry season (37.4%) compared to the long (29.7%) and short rainy seasons (32.9%). Conversely, trees emitted 35.78 t of BVOCs annually, with monoterpene and isoprene being nearly equal contributors. Eucalyptus genus, Casuarina equisetifolia, and Schinus molle species were the top BVOC emitters despite their low population percentages in the study area. While GI types such as urban parks and institutional compounds are effective at pollutant removal, they also exhibit higher BVOC emissions. Our findings highlight the need for optimized species selection, improved GI planning, and enhanced policy support to maximize GI effectiveness, providing valuable insights for planners and policymakers in integrating GI into urban spatial planning.

1. Introduction

Over the next three decades, the world will experience continued urbanization, with the urban population projected to grow from 56% in 2021 to 68% by 2050, adding 2.2 billion population (United Nations Human Settlements Programme, 2022). This rapid urbanization, driven largely by economic opportunities, has led to increased urban expansion, which has significant environmental consequences, including air quality degradation. Despite occupying only 3% of Earth's land surface (Kim, 2018), cities are among the human-modified systems responsible for global air pollution. As cities grow and human activities intensify, air pollutants such as carbon monoxide (CO), ozone (O_3), sulfur oxides (SO_2), nitrogen oxides (NO_2), and particulate matter (PM)) with a diameter ≥2.5 μm (PM2.5) and ≤10 μm (PM10) are primarily emitted by human activities, leading to the deteriorating urban air quality. Pollutant concentration levels in urban centers often exceed the World Health Organization's (WHO) air quality guidelines, posing serious risks to human health (McMichael, 2000). As a result, air pollution contributes to approximately 7 million premature deaths annually, with 4.5 million directly attributed to it and the rest linked to indirect factors (Ouyang et al., 2022). Although no country globally meets the WHO's air quality guideline standards, indicating a widespread health risk (Hewitt et al., 2020), the problem is particularly acute in the Global South (Ouyang et al., 2022) due to a high number of private vehicles and inadequate waste management practices (Amegah & Agyei-Mensah, 2017).

In response to these challenges, integrating Green Infrastructure (GI) into urban areas has emerged as a crucial strategy for improving air quality and mitigating pollution. Urban GI systems refer to strategically planned natural and semi-natural areas, including parks, gardens, forests, green roofs/walls, river-side green spaces, street trees, and institutional compounds, designed to provide multiple benefits (European

☆ This paper has been recommended for acceptance by Dr Alessandra De Marco.

* Corresponding author.
E-mail address: gertik@uni-bonn.de (T. Gebreyesus).

https://doi.org/10.1016/j.envpol.2024.125244
Received 6 September 2024; Received in revised form 15 October 2024; Accepted 3 November 2024
Available online 4 November 2024

Union, 2013; Fairbrass et al., 2018). By integrating GI into urban landscapes, cities can effectively improve air quality through various mechanisms. For example, plants primarily absorb gaseous pollutants through their leaf stomata, with some being intercepted on plant surfaces (Hewitt et al., 2020). In addition, PM settles on leaf surfaces where they may either be absorbed or undergo reactions with other compounds, resulting in the removal of these pollutants (Bottalico et al., 2016). Urban trees are particularly effective at reducing O_3 and SO_2 during the daytime in the growing season when trees are actively transpiring water, whereas trees remove PM and CO both day and night, throughout the entire year, because these pollutants are captured by their leaves and bark (Nowak et al., 2018a,b).

However, it is important to note that urban trees also emit biogenic volatile organic compounds (BVOCs), which can contribute to exacerbating the poor air quality in cities. Some BVOC types such as isoprene (C5H8) and monoterpenes (C10 terpenoids) can react with NOx at high temperatures in the atmosphere to form secondary pollutants, such as ground-level O_3 and CO (Baró et al., 2014; Nowak, 2020a). The emission of BVOCs and their role in O_3 formation vary with environmental conditions and tree species (Calfapietra et al., 2013). Monoterpenes are emitted continuously both day and night, whereas isoprene is released only during daytime when photosynthesis occurs (Benjamin & Winert, 1998). Moreover, monoterpene emissions are temperature-dependent, while isoprene emissions are influenced by both temperature and light conditions (Benjamin & Winert, 1998). These complexities highlight the importance of careful tree selection and GI planning to maximize air quality benefits while minimizing the adverse impacts of BVOC emissions (Isaifan & Baldauf, 2020).

Numerous studies worldwide highlight the air quality benefits of GI, positioning green spaces as essential components of urban spatial planning. For instance, a study by Yao et al. (2022) in Guangzhou, China, estimated that urban trees and shrubs removed 78,481 metric tons (t) of air pollutants (CO, NO_2, O_3, $PM_{2.5}$, and SO_2) annually. Similarly, a study conducted in the Municipality of Ferrara, Italy, revealed that GI elements removed 8.6 t of O_3 and 19.78 t of PM_{10} annually, while an assessment in Beijing, China, showed that urban forests could remove about 17,747 t of NO_2 annually (Muresan et al., 2022; Gong et al., 2022). Moreover, a study by Parsa et al. (2019) demonstrated that urban forests in Tehran, Iran captured 238.4 t of air pollutants annually. An analysis of various types of urban green spaces in China also estimated that GI could remove a total of 92 t of air pollutants annually (Song et al., 2020), and in Brimbank, Australia, industrial zone green spaces eliminated 577 kg $yr.^{-1}$ pollutants (Jayasooriya et al., 2017). Together, these studies underscore the critical role of urban GI in mitigating air pollution, highlighting the need for its integration into urban planning efforts.

In Africa, however, GI elements are not systematically integrated into urban spatial planning, despite its profound benefits for sustainable urban environments (Anderson et al., 2022). In Ethiopia, empirical evidence demonstrating the effectiveness of GI in improving air quality is still lacking. This knowledge gap, coupled with inadequate green space coverage in urban centers—often below 1 m^2 per person compared to the WHO's recommended 9 m^2—worsens environmental and public health challenges (World Bank, 2017). Rapid urbanization and the failure to integrate GI into spatial planning further contribute to declining air quality and undermine sustainability efforts (Lindley et al., 2015). Although promising initiatives like the 'Green Legacy' program exist, they lack the strategic insight needed to optimize environmental benefits and mitigate potential drawbacks, such as BVOC emissions. The existing green spaces in Ethiopia's urban centers, including those in Hawassa, are poorly planned and insufficient to address the high levels of air pollutants the cities encounter (Fetene & Worku, 2013). The lack of research on the trade-offs associated with GI benefits may contribute to suboptimal planning and decision-making, resulting in less effective management of green spaces. Although previous studies have assessed air pollutant concentration in Hawassa (Kasim et al., 2018) and human-induced VOC emission (Amare et al., 2023), the amount of air pollution that could be annually removed and BVOCs emitted by existing GI elements in Ethiopia remains unknown.

This knowledge gap highlights the need for systematic research to demonstrate the roles of GI in improving air quality. Therefore, this study aims to evaluate the effectiveness of GI planning as an air quality improvement strategy in Hawassa, Ethiopia, and specifically to 1) quantify the amount of air pollution annually removed by the existing green spaces and subsequent monetary values; 2) evaluate the BVOC emission rate of tree species; and 3) map the potential pollution interception and BVOC emissions across the city. Our findings will enable planners and policymakers to better integrate GI into urban development strategies to improve air quality and promote sustainable urban growth.

2. Materials and methods

2.1. Study area

This study was conducted in Hawassa, the capital of the Sidama Regional Government in southern Ethiopia. Hawassa spans both midland (1800–3200 m above sea level [m.a.s.l]) and lowland (1500–1800 m.a.s.l) agro-environment (Yona et al., 2024). The city administration, geographically located between 7°03′43.38″ latitude and 38°28′34.86″ longitude, covers 828,260 ha, with the urbanized region spanning about 5200 ha (Tessema et al., 2024, Fig. 1). As a rapidly growing medium-sized city, it is the sixth-largest urban center in Ethiopia, with a population of 351,469 and an annual growth rate of 4%, according to the 2015 census (Scott et al., 2016).

Hawassa's climate, classified as 'Woyina Dega,' features two distinct rainy and dry seasons. The main rainy season occurs from June to September, while a shorter one spans from March to May. The dry season, known locally as "Bega," lasts from late October to February. The city receives an average annual rainfall of approximately 1013 mm and experiences average temperatures of 23.75 °C, ranging from a winter low of 6 °C to a summer high of 34 °C. Monthly average temperatures fluctuate between 10 °C and 31.5 °C (Yona et al., 2024). According to the Federal Urban Planning Institute (FUPI), wind direction shifts from southwest to northeast during the summer and from west to east during the dry season (FUPI.2006). Wind speeds also vary seasonally, with the windiest period from mid-June to late August and the calmest stretch from September to mid-June (Weather Spark, 2021).

2.2. Database customizing and model configuration

We employed the i-Tree Eco Model version 6.0 (Eco v6.0) to assess air pollution removal, its economic value, and BVOC emissions from certain tree species in the study area. The model features a comprehensive database designed to store geographical, meteorological, and air pollution data for cities worldwide (i-Tree Database, 2020). Originally developed by the USDA Forest Service, the model takes into consideration the distinct climate characteristics of the cities in the U.S. Therefore, we manually input location information, meteorological data, and pollution data for the study year into the databases (Yao et al., 2022). We acquired pollutant concentration and precipitation data from the Ethiopian Federal Meteorological Agency following a formal request. Furthermore, the database included only 6500 tree species, and we found that Ethiopia's native species were missing (i-Tree Database, 2020). Therefore, we identified and added these missing species along with their morphological characteristics, guided by Bekele-Tesemma (2007; Fig. 3). Next, we adjusted the frost-free period from the default of 124 days–365 days and modified the allometric equation to a tropical one to better reflect the local climate of Hawassa, Ethiopia. Additionally, we integrated local variables such as temperature and precipitation, which directly influence air pollution removal through the dry deposition process modeled by Eco v6.0 (i-Tree Eco, 2020c). The primary

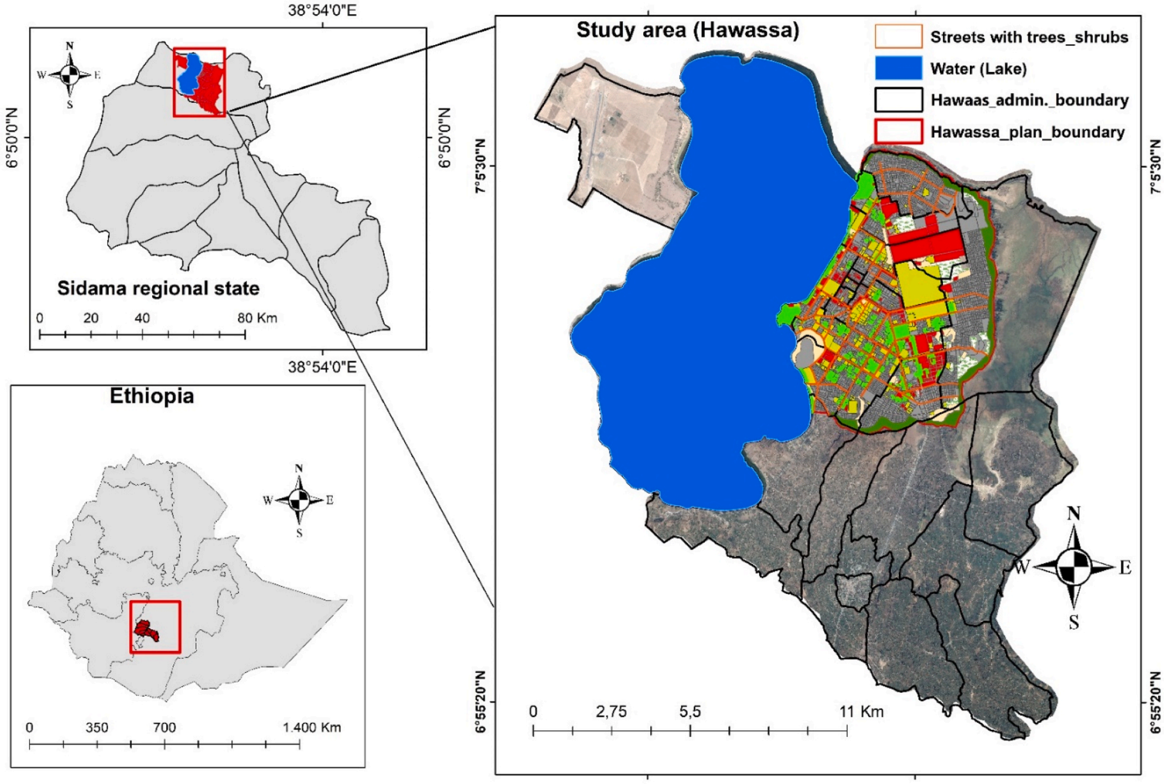

Fig. 1. Location of Hawassa, illustrating the planned development boundary and the administrative boundary, where there is no development plan in the natural area.

purpose of these adjustments was to develop a methodology tailored to the study area and improve the accuracy of the model's analysis output.

We sourced population data, average temperature, and land use information from the municipality of Hawassa. We also obtained geospatial land use data, including land use strata for the entire study area, and incorporated all this information into the model (FUPI, 2006; Hawassa City Administration, 2017). After importing all necessary data into the database, configuring the model, and completing field data entry, the Eco v6.0 project was submitted to the U.S. Forest Service for validation. Upon validation, the project was returned for further analysis (i-Tree Eco, 2020c, Fig. 3).

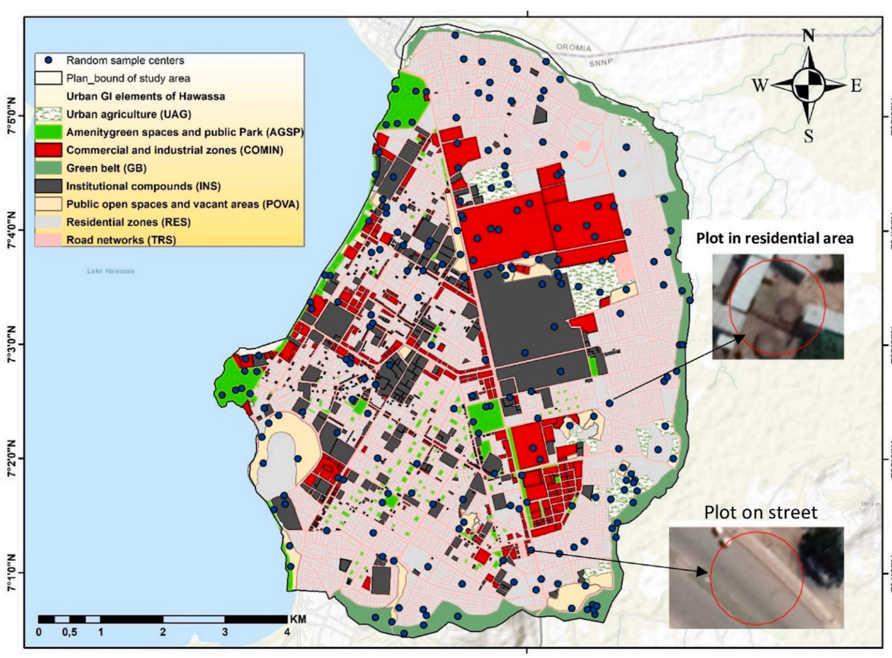

Fig. 2. Urban green infrastructure systems were grouped based on their similarities within the planned boundary, with random sample center plots randomly distributed across each stratum. (For interpretation of the references to colour in this figure legend, the reader is referred to the Web version of this article.)

2.3. Sampling design and sample size

We employed a stratified random sampling design, where the entire city was divided into strata based on the updated geospatial land use data (Fig. 2 and 3). Similar land uses were clustered into eight groups: 1) AGSP - amenity green spaces around neighborhoods, lakeside, gardens, and parks 2) COMIN - commercial and industrial zones, 3) GB - green belt with no management intervention at the periphery, 4) INS - institutional compounds including government and religious compounds, 5) POVA – undeveloped or vacated open spaces, 6) RES - communal and single-family residential areas, 7) TRS: transport corridors such as bus stops, residential roads, main streets, and highways, and 8) UAG: areas zoned as urban agriculture (Fig. 2). Subsequently, center points for each stratum were generated and imported into the model along with the strata shapefile (i-Tree Eco, 2020b). As a rule of thumb, estimating the structure and function of an urban forest for an entire city requires a minimum of 200 random plots, with at least 10 plots per stratum. If some plots are located in inaccessible areas where data collection is impossible, an additional 10% of plots is needed to ensure sufficient data can be collected. Each plot is buffered with an 11.34 m radius to cover the minimum plot area of 400 m^2 (i-Tree Eco, 2020b). We found three of our random sample plots were located within prohibited institutional areas during data collection, rendering them inaccessible. As a result, data collection was accomplished within 217 random plots, exceeding the minimum sample size. This adjustment ensured that the final sample remained representative of the urban forest while adhering to the model guidelines, thus supporting consistency and comparability with other research efforts (i-Tree Eco, 2020b). Before heading to the field, we conducted geospatial quantification using high-resolution images from Google Earth to identify land use, land cover types, and cover proportions at the plot level. These estimates were validated through field measurements within each random plot.

2.4. Field data collection

In each plot, data on trees and shrubs, general plot characteristics, and ground cover information were recorded (i-Tree Eco, 2020b, Fig. 4). Land use was categorized by recording specific types of plots that fell under a single land use category (e.g., commercial area) and noting the percentage of each land use for plots with multiple purposes. Tree canopy cover (TCC), which refers to the percentage of the plot shaded by tree crowns, was estimated through a combination of image analysis and visual observation. High-resolution images were used to determine the canopy cover percentage at the plot level, and these estimates were verified with direct field measurements (i-Tree Eco, 2020b). This estimation involved visualizing the portion of the plot shaded by trees when the sun was directly overhead, with percentages ranging from 0% (no cover) to 100% (full cover). The overall canopy cover for the entire

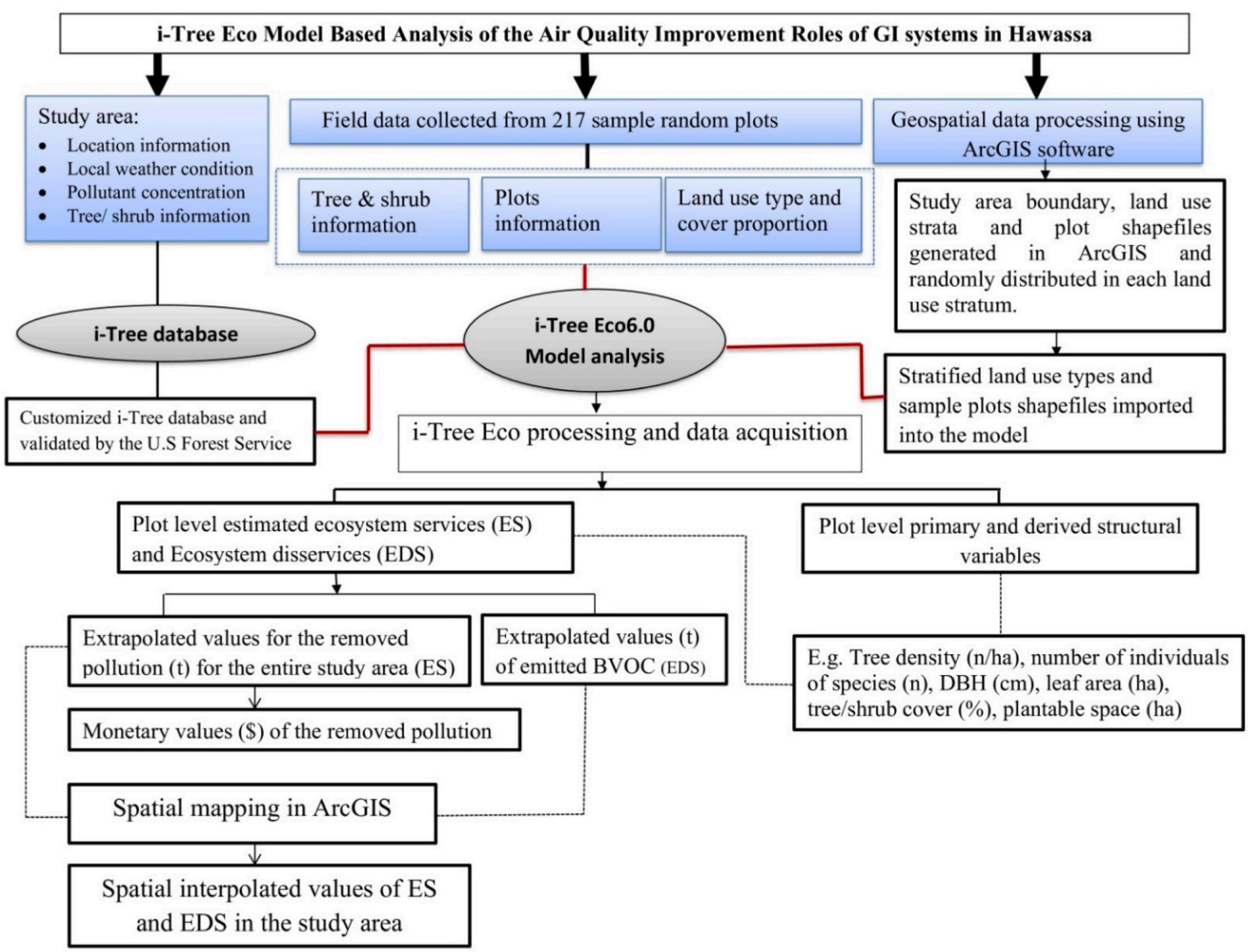

Fig. 3. The Methodological framework of the research integrates i-Tree database customization using rainfall and pollution data, tailored to the city's climate, for assessing air pollution removal, and BVOC emissions by GI systems.

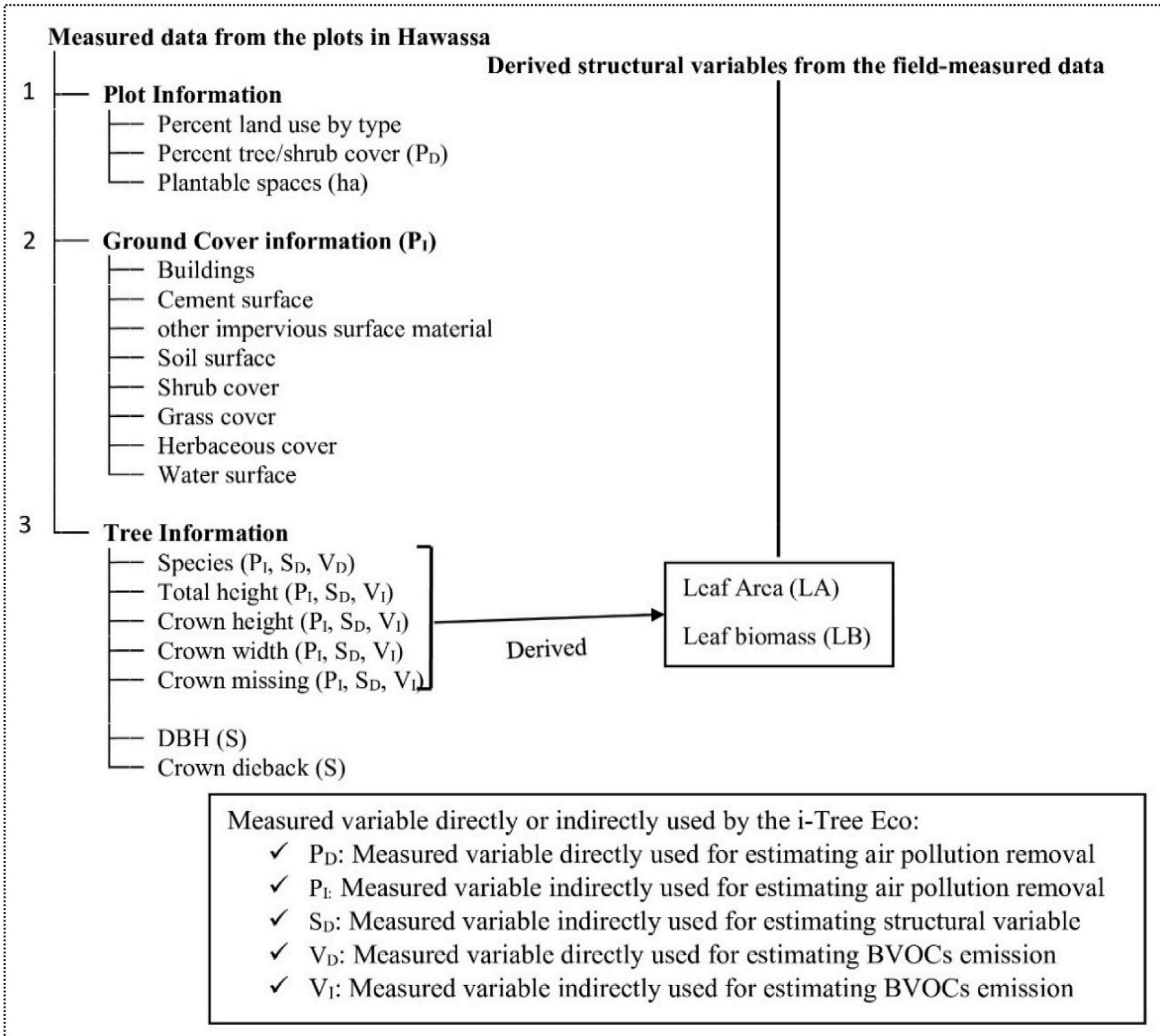

Fig. 4. Overview of major field-measured data from the random sample plots required to quantify the derived variables, air pollution removal, and BVOC emission in the i-Tree Eco (i-Tree Eco, 2020).

study area was extrapolated from the sample plot data using the built-in statistical algorithms of i-Tree Eco (Xie et al., 2023). The computational methods (algorithms) in the model utilize tree characteristics such as canopy spread, diameter at breast height (DBH), and total height to estimate total canopy cover and other related metrics (i-Tree Eco, 2020b).

The common, scientific, and local names of each tree and shrub species in the sample plots were identified during the field survey with the assistance of foresters and botanists. Moreover, we cross-referenced the tree species with Bekele-Tesemma (2007), thoroughly reviewing their origins, leaf types (deciduous, evergreen, broadleaf, coniferous), and other relevant characteristics. Other measurements, such as DBH for single-stemmed trees and the DBH of each stem for multi-stemmed trees, were taken using calipers. Total tree and bole heights were measured using a clinometer and a wooden stick, respectively. The crown width was determined by measuring the diameters of the crown in both the north-south and east-west directions. We assessed the percentage of foliage lost due to pruning, dieback, defoliation, uneven crowns, or the presence of dwarf or sparse leaves to estimate the canopy missing. These field-measured structural variables within the sample plots were extrapolated to citywide based on our configuration and were used to compute derived variables like leaf area (LA) and leaf biomass (LB) using regression equations (Nowak, 2020a, Fig. 4). The LAI was estimated from field-collected data using UFORE-A, a program that works in conjunction with UFORE-D within the Eco 6.0 model, where regression equations are applied to estimate the LA of individual urban trees (Hirabayashi et al., 2012).

2.5. *Air pollution removal, economic value, and BVOC emission analysis*

Hourly removals of CO, NO_2, O_3, SO_2, PM_{10}, and $PM_{2.5}$ throughout the year were estimated using the dry deposition model, which is an integral part of Ecov6.0 (Nowak et al., 2008). The pollutant flux (F in μg m^{-2} h^{-1}), which represents the density of gaseous pollutants at the vegetation surface, is calculated according to Baldocchi et al. (1987):

$$F = V_d \, x \, C \tag{1}$$

Where C represents the concentration of pollutants (μg m^{-3}) and V_d is the dry deposition velocity of pollutants (cm s^{-1}), a process influenced by pollutant characteristics, wind speed, and direction, and the canopy surface properties (Hewitt et al., 2020). V_d is calculated using the individual resistances of pollutant transfer to tree surfaces: aerodynamic (R_a), quasi-laminar boundary layer (R_b), and canopy resistance (R_c), where Ra represents air movement resistance within the crown space (s m^{-1}), R_b is the transfer resistance through the boundary layer adjacent to canopy surfaces (s m^{-1}), and R_c denotes the chemical and biological absorption capacity canopy surfaces (s m^{-1}) (Hirabayashi et al., 2012).

$$\mathrm{Vd} = \frac{1}{Ra + Rb + Rc} \quad (2)$$

The values and calculation procedures for R_a, R_b, and R_c are detailed in (Hirabayashi et al., 2015; Nowak, 2020a). The capacity of individual trees to filter pollutants is calculated using the formula:

$$P_{rem} = R_t x \left(\frac{LA_x}{LA_t} \right) \quad (3)$$

P_{rem} is pollution removal by a certain tree (kg), R_t represents the total pollution removed for all trees (kg), LA_x represents the total LA of a certain tree (m^2), and LA_t is total LA of all trees (m^2). LA is the total surface area (one-sided) of the leaves on a tree, whereas LAI is the total LA per unit of ground surface area (Nowak, 2020a) and can be calculated according to the equation detailed in Hirabayashi et al. (2012):

$$LAI_i = \frac{LA_i}{A_i x TC_i} \quad (4)$$

Where LA_i, A_i, and TC_i represent the LA (ha), ground area (ha), and TCC (%) for land use type i, respectively. The LA of individual open-grown trees is determined using regression equations specific to urban trees (Nowak et al., 2008):

$$\ln Y = -4.3309 + 0.2942H + 0.7312D + 5.7217S + -0.0148C \quad (5)$$

Y represents LA (m^2), H is the crown height (m), D is the average crown diameter (m), S is the average shading coefficient factor for the individual species, and C is the crown surface area (m^2).

Furthermore, we conducted a spatial analysis based on the Ecov6.0 model analysis outputs by integrating the information into GIS software. All the sample plots from which we collected the required data were included in the spatial analysis. Data from the sample plots randomly distributed such as the amounts of removed air pollutants, BVOC emission, LAI, TCC values, and corresponding geographical coordinate systems were exported from the model and imported into ArcGIS for further analysis. The Empirical Bayesian Kriging method in ArcGIS is an accurate method for analyzing the structure and function of urban forests (Yang et al., 2023). Likewise, Xie et al. (2023) evaluated four interpolation methods for spatially interpolating ecosystem services and found that Kriging had the highest prediction accuracy. Therefore, we used the Kriging method in ArcGIS (version 10.8) for spatial interpolation to map the estimated annual air pollution removal, emitted BVOC, and structural variables such as LAI and TCC.

The economic value attributed to removing pollutants annually depends on the population benefiting from improved air quality (Nowak et al., 2018a,b). We employed the externality values, which estimate the social cost of air pollution not captured in market prices and include its adverse effects on human health, the environment, and man-made materials (Nowak et al., 2014a,b). Ethiopia currently lacks comprehensive data on the social costs of air pollution, with limited information on its full economic, health, and environmental impacts. Thus, we used periodically updated U.S. median externality values—\$1518.4/t for CO, \$10691.2/t for NO_2 and O_3, \$7138.05/t for PM10 and PM2.5, and \$2617.31/t for SO_2—to estimate the monetary value (Nowak et al., 2014a,b).

The emission of BVOC types, such as isoprene and monoterpenes, is calculated for each tree species. BVOC emission rates depend on tree species, leaf biomass, and air temperature (Nowak et al., 2008). Thus, genera-specific emission factors based on the proportion of biomass of species within the genera are used to estimate emissions of individual species (Nowak, 2020a). The BVOC emission (E in μgC/hr) for each tree species is estimated as:

$$E = BE\ x\ B\ x\ \gamma \quad (6)$$

Where B represents the leaf dry weight biomass (g), BE is the genus-specific emission factor (μgC/g) from literature at a temperature of 30 °C and photosynthetically active radiation (PAR) flux of 1000 μmol/m^2/s. In the absence of genus-specific information, existing median BE values from families in the literature are used. Similarly, tropical allometric equations from the literature were used to estimate the total tree biomass (Nowak, 2020a). The equations to estimate γ (temperature and light correction factor) for both BVOC types are detailed in Nowak (2020a), while PAR calculations are based on Nowak et al. (2008).

3. Results

3.1. Structure of the GI systems in Hawassa

The entire urban greenery of Hawassa comprises 20.7% tree and 3.7% shrub cover, with trees predominantly featuring 53% evergreen broadleaved, 40% deciduous broadleaved, and 7% coniferous. About 70% of trees have a DBH of less than 15 cm, 26.4% fall within the DBH class of 15.2–44.7 cm, and 3.4% exceed 45 cm. Besides, tree cover varies substantially across different GIs, ranging from 11.9% in GB to 44.1% in AGSP. Although RES has the least tree cover, it exhibits a higher LAI, surpassed only by INS, while the lowest LAI values were recorded in UAG and POVA (Table 1). Moreover, approximately 2064 ha of land in Hawassa supports tree growth, with significant portions of UAG, GB, and AGSP offering higher plantable spaces, while TRS and COMIN showed limited plantable space.

The spatial distributions of LAI and TCC reveal a clear association with air pollution, with higher LAI values in the northern and southwestern part of the city aligning with areas of dense canopy cover, particularly in enclosed parks and Hospital compounds (Fig. 5). In these regions, LAI values exceed 3 (indicated by dark green), corresponding with areas of higher vegetation density. Similarly, the TCC spatial map highlights the same regions as having the densest canopy cover, with values reaching up to 70% in the areas where closed parks, gardens, and institutions are prevalent. In contrast, the central part of Hawassa features a mix of LAI values between 1 and 3 (Fig. 5a). The less urbanized eastern part, characterized by scattered settlements, shows the lowest LAI values (<0.5), while the TCC map reflects scattered lower canopy cover percentages (10–30%) (Fig. 5b). The alignment of LAI and TCC, both estimated using the same method in spatial analysis, reinforces the consistency of these critical indicators of vegetation health and ecosystem function. Additionally, our field validation enhances the precision of information and the reliability of the methodology employed.

3.2. Air pollutant removal and economic values

The urban trees and shrubs in Hawassa removed 274.2 t per year (t $yr.^{-1}$) of CO, NO_2, O_3, SO_2, PM_{10}, and $PM_{2.5}$, with an economic value of \$1.79 million. Trees accounted for 83.4% of this removal, while shrubs contributed 16.6%. Among the pollutants, SO_2 accounted for about 45% (122.5 t) of the annual removal, followed by O_3 (79.9 t) and NO_2 (32.1 t). In contrast, pollutants such as CO, $PM_{2.5}$, and PM_{10} were the least removed, with total annual removal values of 5.4 t, 17.21 t, and 17.27 t, respectively. Similarly, the highest annual mean removal was observed for SO_2 at 40.9 ± 1.8 t, followed by O_3 at 26.6 ± 1.4 t, whereas CO, PM_{10}, and $PM_{2.5}$ had still lower mean removal rates (Fig. 7a). Standardizing the average removal rate by tree cover, a square meter of TCC in the entire study area could remove 21.3 g m^{-2} $yr.^{-1}$. At pollutant level, SO_2 (11.4 g m^{-2}), O_3 (7.4 g m^{-2}), and NO_2 (3 g m^{-2}) were removed at the highest rates compared to CO (0.5 g m^{-2}), PM_{10} (1.51 g m^{-2}), and $PM_{2.5}$ (1.6 g m^{-2}). However, the greatest monetary values derived from the removal were recorded for O_3, followed by NO_2 and SO_2, with removal values in thousands being \$864, \$347, and \$325, respectively. The remaining removal monetary values were contributed by PM (\$250,000) and CO (\$8318).

Table 1
Summary of structural variables, total annual and average annual air pollution removal rates, and corresponding monetary values (in thousands) quantified for each GI type in Hawassa.

GI type[a]	Tree density (N/ha)	LAI	Coverage proportion			Pollution removal		Total value ($)
			Plantable space (ha)	Tree (%)	Shrub (%)	Total (t yr^{-1})	Average (g m^{-2} $yr.^{-1}$)	
UAG	190.29	0.7	133.50	17.20	2.90	5.80	20.20	37.60
AGSP	165.32	3.5	83.10	44.10	5.30	33.80	39.30	220.60
COMIN	41.75	0.4	229.80	15.20	6.30	12.50	12.20	81.80
GB	114.95	0.4	233.30	11.90	8.00	5.90	16.60	38.50
INS	115.31	2.4	736.70	34.80	2.80	85.60	34.10	559.40
POVA	89.24	0.7	74.70	19.90	4.20	7.40	18.30	48.20
RES	120.46	0.6	736.70	18.90	2.80	56.30	15.10	367.70
TRS	115.07	0.5	308.30	16.40	2.70	21.50	13.60	140.40

[a] UAG: Urban Agriculture, AGSP: Amenity Green spaces along lakeside, neighborhood green areas, and Public Parks, COMIN: Commercial and Industrial Areas, GB: Green Belts, INS: Institutional compounds, POVA: Public Open Spaces and Vacant Area, RES: communal housing and Single-family residential areas, TRS: Transportation corridors, including bus station and streets.

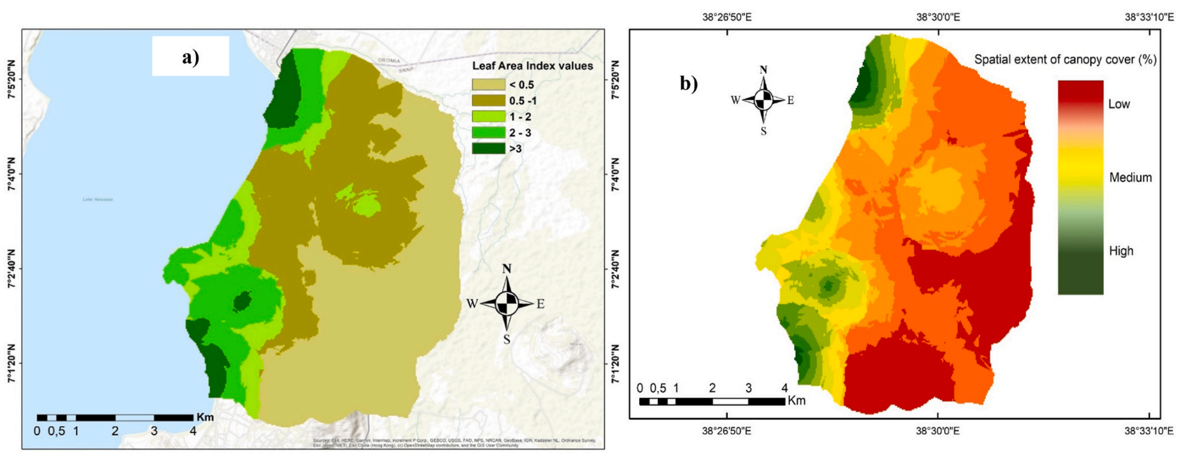

Fig. 5. The spatial distribution of the LAI ranging from high vegetation coverage in parks and gardens to low foliage cover in recently urbanized areas with fewer green spaces (a), while the spatial extent of TCC, aligned with the LAI, providing a comprehensive overview of tree cover variability across different locations (b). (For interpretation of the references to colour in this figure legend, the reader is referred to the Web version of this article.)

3.3. Spatial and seasonal variation

Annual air pollution removal and associated monetary values in Hawassa ranged from 5.8 t $yr.^{-1}$ ($37.6 thousand) in UAG to 85.6 t $yr^{-}.^{1}$ ($559.4 thousand) in INS. Higher air pollution reduction occurred in RES, followed by AGSP and TRS, while GB, POVA, and COMIN had the lowest removal values (Table 1). Similarly, average removal rates varied across land use types, ranging from 12.2 g m^{-2} $yr.^{-1}$ in COMIN to the highest value of 39.3 g m^{-2} $yr.^{-1}$ in AGSP. The spatial analysis revealed that the highest annual removal occurred in areas with large native and broadleaved trees, such as public conservation parks and gardens, while lower removal was observed in less urbanized parts of Hawassa with smaller or sparser green spaces (Fig. 6). The highest and lowest pollution removal capacities of each GI element are associated with the TCC and LAI pattern (Table 1 and Fig. 5).

The air pollution removal efficiency of GI components varied substantially depending on the seasons and specific months (Fig. 7). The greatest removal, amounting to 102.56 t $yr.^{-1}$, occurred during the driest season, followed by the short rainy season with an estimated value of 90.25 t $yr.^{-1}$. The long rainy season, with the lowest temperatures and higher wind speeds, showed the lowest removal at 81.35 t $yr.^{-1}$. November (36.93 t) and December (29.63 t), the driest months, had the highest cumulative air pollution removal across all the pollutants, with May, March, and April following closely with estimated removals of 23.2 t, 22.9 t, and 22.5 t, respectively. August, a typical wet and windy month, recorded the lowest pollution removal at 17.9 t (Fig. 7b). During the short rainy season, PM_{10} removal was negligible (Fig. 7a), while $PM_{2.5}$ showed a negative removal value in December, which is the windiest month in Hawassa. The negative value indicates that the resuspension of previously settled PM_{10} by trees exceeds the rate at which it is being removed. NO_2 removal peaked during the driest season, with November and December showing the highest removal values at 15.2 t and 13.6 t respectively, and lower removals in the rainy months. Similarly, O_3 removal varied from 5.11 t in August to 8.81 t in December, while CO removal remained consistently low throughout the year, highlighting the significant seasonal variability in pollutant removal rates in Ethiopia (Fig. 7b).

At the species level, *Ficus sur* and *Grevillea robusta*, followed by *Jacaranda mimosifolia* and *Azadirachta indica,* were the top contributors to the annual air pollution removal, collectively accounting for approximately 48% of the total removal in Hawassa. In contrast, *Bersama abyssinica, Prunus persica, Podocarpus falcatus, Carissa spinarum, Citrus sinensis,* and *other* small trees demonstrated nearly zero removal value. Averaging the annual air pollution removal per tree (kg/Tr.), *F. sur* is still at the top with 11.39 kg, followed by *Ficus vasta* (5.11 kg), *Acacia tortilis* (1.17 kg), *Senna siamea* (0.95 kg), and *Moringa oleifera* (0.92 kg) (see Appendix 1 for more details).

3.4. BVOCs emissions

We found that BVOC types such as monoterpenes (49.7%) and isoprene (50.3%) emitted in similar proportions. The entire urban forests of Hawassa could emit 35.8 t BVOC, of which the highest emissions were recorded in INS (12.06 t $yr.^{-1}$) and RES (7.24 t $yr.^{-1}$), and the

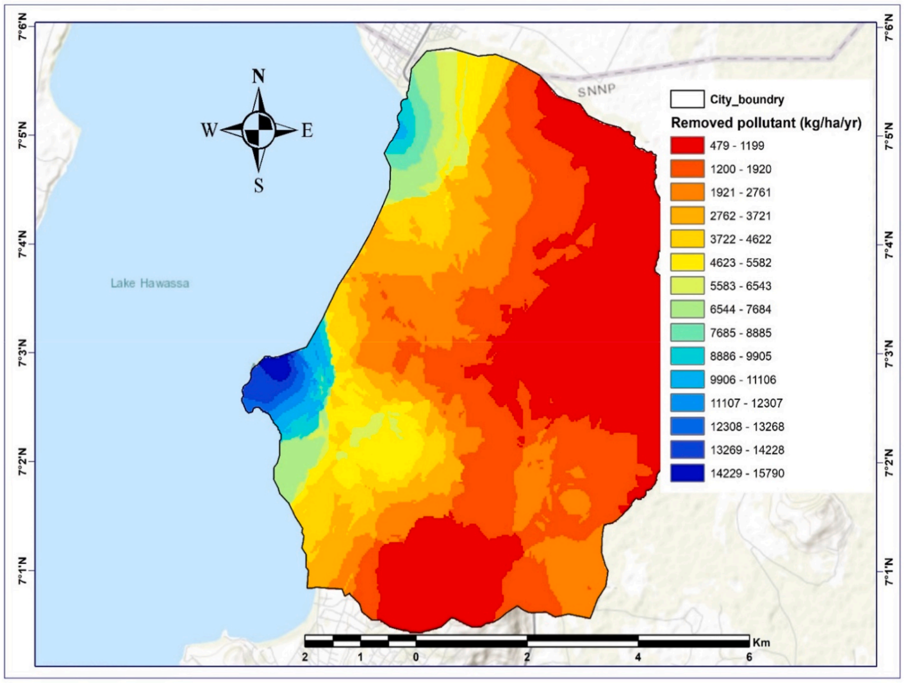

Fig. 6. Spatial distribution of annual air pollution removal by different GI types across land use categories highlights areas of both substantial and minimal pollution removal.

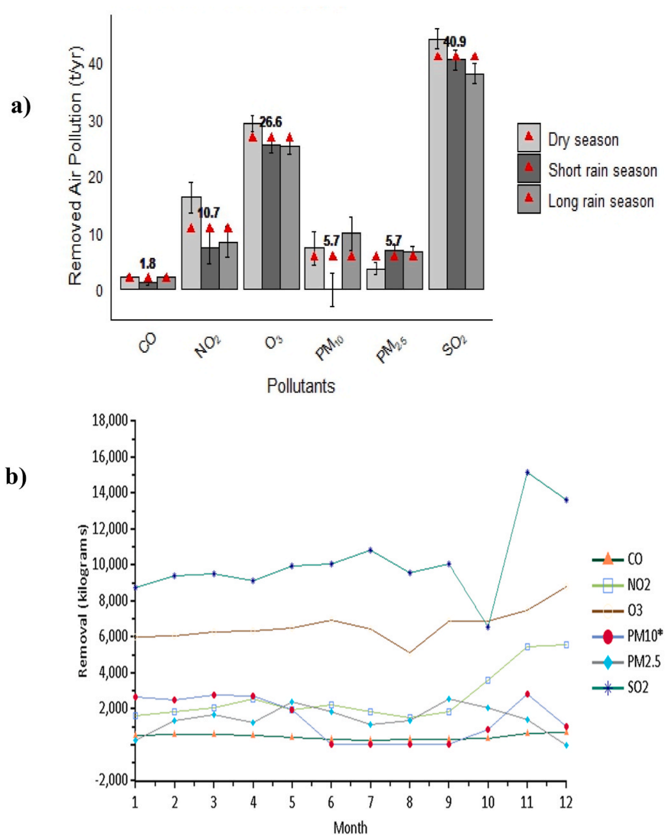

Fig. 7. Seasonal variation air pollution removal: a) total air pollution removed across the three major seasons, with a mean removal rate (Mean ± SE) of pollutants (red triangles), and b) monthly variation in total annual pollution removal (kg) for each air pollutant from January to December across the existing GI systems in Hawassa. (For interpretation of the references to colour in this figure legend, the reader is referred to the Web version of this article.)

lowest annual emissions were contributed by UAG and GB (Table 2). Yet, the average annual BVOC emission rate per m^2 of tree cover varied considerably, with higher values in POVA, and GB, while RES, TRS, and UAG similarly showed the lowest average emissions (Table 2). The BVOC emissions for all tree species, ranked according to their emission levels per LB (kg) and LA (ha) are summarized in Appendix 1. In terms of BVOC annual emissions, *F. sur* and *Eucalyptus camaldulensis* were identified as the highest emitters, each contributing 7.7 t $yr.^{-1}$ (21.4%). However, emission rates varied considerably among tree species, when averaged for BVOCs by LA and LB. The *Eucalyptus* genus emerged as the highest average BVOC emitter, with *E. camaldulensis* and *Eucalyptus citriodora* annually emitting 58.8 and 56.04 kg per ha of LA, respectively. Moreover, *Casuarina equisetifolia and Schinus molle* demonstrated relatively higher BVOC emissions per ha of LA. Despite *F. sur* having the highest total emission, its average emission rate per ha of LA was the lowest at 8.7 t $yr.^{-1}$. Spatially, the highest emissions were recorded in the conservation parks where these trees are found predominant (Fig. 8). A minor shift was observed in the average BVOC emission rate when averaging the values by LB (grams of BVOC per kg of LB). Thus, *C. equisetifolia* exhibits the highest average emission rate, at 49.1 g/kg/yr. of LB, closely followed by *E. citriodoraand* and *E. camaldulensis* at

Table 2
i-Tree Eco-based total (t $yr.^{-1}$) BVOCs emission quantified for each GI type established across various land use types and the average emission (g m^{-2} $yr.^{-1}$) by square meter of tree canopy cover in Hawassa.

Stratum	TCC (ha)	Monoterpenes (t $yr.^{-1}$)	Isoprenes (t $yr.^{-1}$)	BVOC emission		
				Total (t $yr.^{-1}$)	TCC (g m^{-2} $yr.^{-1}$)	%
INS	251.4	5.20	6.86	12.06	4.80	33.70
RES	373.3	4.52	2.72	7.24	1.94	20.23
AGSP	86.0	1.67	2.50	4.17	4.85	11.65
COMIN	103.1	2.07	2.09	4.16	4.04	11.63
TRS	157.5	2.00	1.23	3.23	2.05	9.02
POVA	40.4	0.89	1.55	2.44	6.03	6.81
GB	35.5	1.16	0.66	1.82	5.13	5.08
UAG	28.6	0.28	0.39	0.67	2.36	1.88

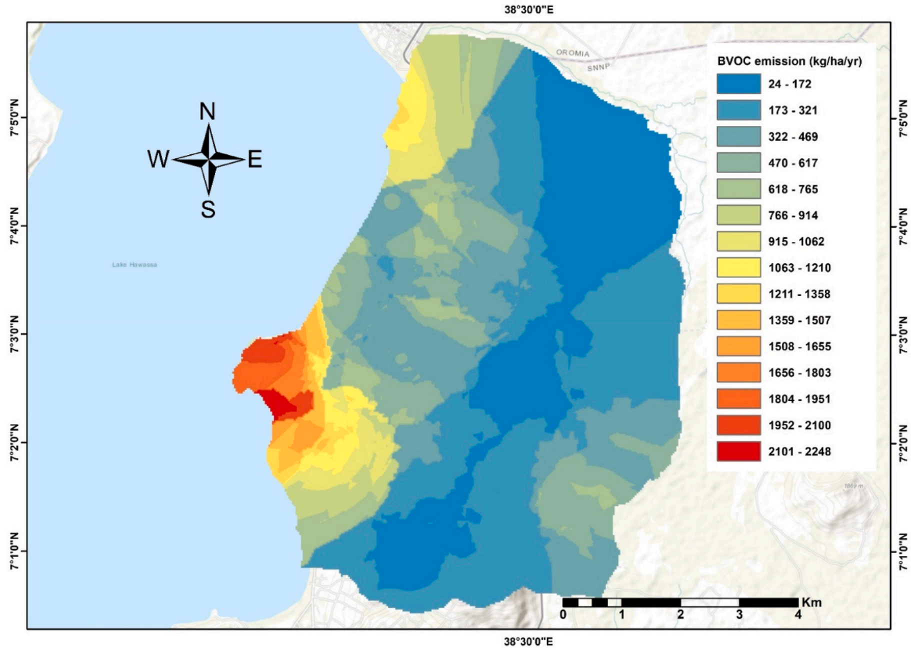

Fig. 8. Spatial distribution (highly concentrated at the recreational and conservation parks and reduced towards the less urbanized part of the city) of the annually emitted BVOC by the GI systems in Hawassa.

similar emission rates, indicating a significant emission output relative to their biomass. Conversely, *Annona senegalensis, Carissa spinarum, Cordia africana, Jacaranda mimosifolia, Podocarpus falcatus,* and *Prunus persica,* emitted neither of the BVOC types, while others (e.g. *G. robusta, S. molle)* showed no isoprene emissions.

4. Discussions

Our study assessed four major issues: (1) the air quality improvement provided by urban green spaces through atmospheric impacts, (2) the monetary values of these services, (3) the emission of BVOCs from urban trees, and 4) the spatial patterns of the removed pollutants and emitted BVOCs in relation to the structural variables of GI systems. To understand the broader implications, it is essential to situate the findings within local, regional, and global contexts. Although comparison with local studies is vital, given the unique characteristics of urban centers in Ethiopia and other African regions, a significant gap on this topic persists (Anderson et al., 2022). Our comprehensive analysis serves as a vital starting point for future investigations into how well-planned GI systems can mitigate air pollution in similar urban environments. While regional and global comparisons provide valuable insights, the scarcity of local studies highlights the need for targeted research in Ethiopia.

The notion of urban green infrastructure is increasingly recognized for its potential to improve air quality, a benefit documented in various studies (e.g., Gong et al., 2022; Muresan et al., 2022; Yao et al., 2022). Our findings align with previous studies, indicating that the GI elements in Hawassa removed 274.2 t of pollutants annually. This result is comparable to the 238.4 t of pollution removed by green spaces in Tabriz (Parsa et al., 2019), but approximately three times higher than the 92 t removed by the GIs in Luohe City, China (Song et al., 2020). The GI systems effectively removed gaseous pollutants (SO_2, O_3, and NO_2) primarily through leaf stomata uptake, whereas less efficient against PM and CO, which are mainly removed through deposition on plant surfaces (Hewitt et al., 2020). Our study reveals that the GI systems of the city are more effective in air quality improvement through pollutant uptake via stomata during active photosynthesis than through surface deposition. In contrast to other studies, which often identify SO_2 as one of the least removed pollutants (e.g., Selmi et al., 2016; Yao et al., 2022), our findings indicate that it was removed more efficiently, highlighting the influence of local environmental conditions. Typically, gaseous pollutants were removed at a higher rate during the driest season, starting in late October, with SO_2 and NO_2 showing the greatest removal in October and November. The increased removal of these two pollutants during the driest months aligns with Nowak et al. (2014a,b), suggesting that the deposition rates are linked to high temperature and a relatively high concentration due to low wind speed during these months in Hawassa. Conversely, the negative removal value of PM pollutants in December may be attributed to strong winds, suggesting that the amount of dust and particles resuspended in the air exceeded the amount removed by the trees (Hirabayashi et al., 2015; Rasoolzadeh et al., 2024). Thus, local factors like temperature and wind speed influence GI pollutant removal, enhancing the permanent elimination of gaseous pollutants while contributing to the redistribution of particulate matter.

Determining the percentage of air quality improvement resulting from the total removed air pollution is essential for understanding its environmental benefits. However, the lack of emission data in Hawassa posed challenges in quantifying these improvements, a challenge across Ethiopia (Flanagan et al., 2021). Studies in various countries indicate that the annual air quality improvements from removed pollutants are often below 1%; however, these changes can still greatly impact human health (Nowak et al., 2018a,b). For example, in Strasbourg, public green spaces removed 88 t pollutants annually, resulting in a 0.5% air quality improvement (Selmi et al., 2016), while urban forests in Barcelona removed 305.6 t per year, yielding less than 1% improvement for PM and NO_2 (Baró et al., 2014). These findings indicate that while GIs in different cities may remove varying amounts of air pollution compared to Hawassa, regardless of the amount removed, they can significantly benefit human health.

The air pollution removal capacity of GI can be influenced by seasonal climate, precipitation, evergreen canopy cover, and pollutant concentration. Generally, increases in these factors enhance the effectiveness of GI, although deposition velocities may decrease during high precipitation (Nowak et al., 2006). Therefore, the surface area of green space coverage alone does not ensure consistent air pollution removal efficiency; smaller GIs can achieve a higher average air pollution removal rate per canopy area (Nowak & Heisler, 2010). In our study, we estimated the annual air pollution removal rate per unit area of tree canopy at 21.3 m^{-2} yr^{-1}, comparable to urban forests in Los Angeles (23.1 g m^{-2} $yr.^{-1}$) (Nowak et al., 2006). However, our study's average removal is approximately twice that reported by Rasoolzadeh et al. (2024) in Tehran, Iran (11.6 g m^{-2} yr^{-1}), and Parsa et al. (2019) in Tabriz, Azerbaijan (10 g m^{-2} yr^{-1}). It is important to note that Ethiopia's frost-free climate enables year-round vegetation growth, resulting in robust plant development, especially during the rainy season, which contrasts with findings in non-tropical regions. For instance, research from Baltimore (Hirabayashi et al., 2012) and Chicago (Yang et al., 2008) indicates that GI systems removed more air pollution during frost-free seasons when photosynthetic vegetation is active. However, we observed the lowest air pollution removal during the long rainy season, typically the peak growing period, which is characterized by higher precipitation and lower temperatures (Weather Spark, 2021) that seem to reduce pollution removal. These findings align with Nowak et al. (2018b), who observed that increased precipitation can lead to decreased air pollution removal through dry deposition. Furthermore, the highest temperatures and lowest wind speeds in Hawassa occur during the dry season, resulting in higher pollutant concentrations and deposition velocities (Hirabayashi et al., 2015; Selmi et al., 2016).

This study also confirms that pollution reduction efficiency varies considerably across GI types, with larger leaf surfaces and extensive canopy cover, such as urban parks, showing the highest pollutant removal rate. Institutional compounds and residential areas, which featured the highest LAI, resulted in the most significant pollution reduction. In Ethiopia, GIs around church and institutional compounds typically comprise mixtures of large native broadleaved trees, as they have ample space for large tree growth. Our findings confirm that broadleaved trees, which thrive in areas with ample space, are most effective for air pollution removal. Conversely, smaller ornamental trees and shrubs, commonly found in more confined environments like streets and residential areas, are less efficient. The benefits of green spaces in these areas, which are often dominated by buildings, extend beyond the scope of atmospheric air pollution removal, particularly in reducing building energy use through cooling effects. Consequently, further research should assess how urban trees in Ethiopia can contribute to reducing air pollutant emissions from buildings by absorbing high levels of solar radiation. Standardized average pollution removal provides more meaningful information than total removal comparisons for evaluating the spatial efficiency of GIs in different locations. Our analysis revealed that urban parks and institutional compounds are the most efficient GI types at removing air pollution, with average annual removal rates of 39.3 g m^{-2} and 34.1 g m^{-2}, respectively. Despite higher pollutant concentrations in transportation corridors and industrial areas in Hawassa (Kasim et al., 2018), these GI types showed lower removal rates. Thus, this research strongly recommends increasing the current tree cover—16.4% in TRS, 15.2% in COMIN, and 18.9% in RES—to better accommodate the high pollution concentrations in these areas.

Urbanization patterns significantly influence the balance between green spaces and built-up areas, which affects air pollutant concentrations and the efficiency of pollution removal. This study found higher total air pollution removal in the oldest part of Hawassa, where business districts, institutions, formal residential areas, and well-maintained green spaces are located. This area demonstrates relatively better LAI and TCC compared to the peripheral area in the eastern part (Fig. 5). Similar spatial distribution trends for other ecosystem services, such as temperature and runoff reduction roles of GI have been observed in previous studies in the city (Gebreyesus et al., 2022, 2023). In contrast, urban agriculture and the green belt contribute minimally to air pollution removal, likely due to the predominance of small trees, which create a scattered canopy and low LAI (Fig. 5). Most trees in these GI types fall into the smallest DBH class (<6 cm), resembling bushes more than mature trees (Gebreyesus et al., 2023). Supporting these findings, Isaifan and Baldauf (2020) reported that large, healthy trees with a DBH greater than 76 cm can remove 60–70 times more air pollution annually than small, healthy trees with a DBH less than 7.6 cm (Nowak, 2020b). Moreover, the spatial variation of pollutant removal in this study is closely linked to TCC and LAI distributions. Areas with higher tree canopy cover, such as the southern part of the city with large native trees in Hospital compounds, gardens, and enclosed parks, as well as the northern region, correspond to zones with greater pollutant removal (Fig. 6). The western and northwestern parts of the city, characterized by denser TCC and higher LAI (Fig. 5), show the highest pollutant removal. Tree canopy measures crown volume, but does not directly reflect leaf surface area, which makes its role in air pollution removal less direct than that of LAI. LAI directly measures the leaf surface available for gas exchange and pollutant absorption (Hewitt et al., 2020). Thus, areas with more extensive leaf surfaces are more effective at filtering particulate matter and absorbing gaseous pollutants.

The roles of urban trees in improving air quality can be translated into economic benefits, primarily due to associated improvements in human health (Nowak et al., 2018a,b). The economic value of pollution removal by the urban forests in Hawassa, estimated at $1.79 million reflects a meaningful contribution to environmental benefits in the city. In comparison, a study in Tabriz, Azerbaijan estimated that the city's green spaces provide an annual pollution removal benefit valued at approximately $ 191 thousand, only 10% of the values in Hawassa (Parsa et al., 2019). Similarly, a study conducted in Barcelona, Spain, valued pollution removal at approximately $2.38 million annually, which is 25% greater than the values in our study (Baró et al., 2014). Given that Hawassa is a smaller city with potentially lower overall tree cover and pollution levels, the estimated value seems reasonable. Spatially, most of the economic benefits in Hawassa from air pollutant removal were concentrated in institutional compounds, residential areas, amenity green spaces, and parks. Together, these areas accounted for approximately 77% ($1.15 million) of the total monetary values derived from pollution removal, resulting in healthcare savings. These GI types are the most visited, closest to residents, and interconnected with the day-to-day life of the community. According to Nowak et al. (2014a,b), urban forests' air pollution removal and associated economic value are considerably higher in cities than in suburban areas, due to higher air pollution levels and closer proximity of residents to green spaces. Furthermore, Nowak et al. (2018b) noted that the GI types with the highest air pollution removal rates do not always yield the highest economic benefits. Factors such as the number of people benefiting from improved air quality are important in determining the economic values of GI types. Despite the highest removal quantity being recorded for SO_2, the highest economic values for air pollution purification were noted for O_3 and NO_2. This implies that removing even a small amount of O_3 and NO_2 is highly valuable because changing (lowering) the concentration of these pollutants in the atmosphere might have the greatest externality or health impact (Nowak et al., 2014a,b).

Although urban greenery is traditionally seen as a net positive for air quality, adverse environmental consequences can arise if GIs are established without proper caution, mainly due to BVOC emissions. These emissions can contribute to air quality degradation when BVOCs react with NO_x at high temperatures, leading to the formation of other pollutants. According to Kumar et al. (2019), isoprene contributes to ground-level O_3 formation in the presence of NOx, whereas monoterpenes can lead to increased concentrations of PM. The authors further elaborated that once released into the atmosphere, BVOCs are highly reactive, with atmospheric lifetimes ranging from seconds to hours, and they rapidly react with air oxidants. However, it is important to note that BVOCs themselves are not inherently air pollutants but consist of plant compounds like essential oils and resins that help trees attract pollinators and deter predators (Chaparro & Terradas, 2009). For instance, in rural areas that often experience lower temperatures than urban areas due to higher tree cover and lower NO_x concentrations, BVOCs can reduce O_3 levels (Nowak and Crane, 2000).

Our study confirms that green spaces can influence air quality dynamics, with an annual emission of 35.8 t of BVOCs in the entire urban forest of the study area. Specifically, *Eucalyptus* and *Ficus* genera were found to be the major contributors, together accounting for over 51% of the total emissions. In a similar study conducted in Adama, Ethiopia, it was reported that the entire urban forest could emit 52 t $yr.^{-1}$ (Koricho et al., 2021), which is approximately 31% higher than the emissions in Hawassa. A comparative analysis at the global level shows considerable differences in BVOC emissions across various locations. For instance, in Mexico City, only 0.4 t $yr.^{-1}$ of BVOC was emitted by urban trees in park-like GI type (Baumgardner et al., 2012), substantially lower than the emission level recorded in Hawassa. Conversely, BVOC emissions in Barcelona's Urban forests were much higher, at 184 t $yr.^{-1}$ (Chaparro & Terradas, 2009), reflecting the influence of different urban settings and climatic conditions. Recent studies in Africa, such as Amare et al. (2023) in Hawassa have examined the health risks of anthropogenic VOCs, while Cordell et al. (2021) in Nairobi and Lagos emphasized the need to examine emissions of these chemicals from human activities. However, these studies failed to examine the impact of BVOCs emitted from urban trees and shrubs.

This research further reveals that BVOC emissions are influenced by a range of factors including tree biomass, temperature intensity, and NO_x concentration. In our study, we observed considerable spatial variations in total BVOC emissions that closely reflected the distribution of green coverage, similar to the pollution removal spatial pattern. The spatial overlapping of high pollutant removal and BVOC emissions, as shown in Figs. 6 and 8, is driven by two main factors. First, the areas with denser forest cover, large trees, and high LAI are where the most pollutants are removed. Second, many of the same trees recorded in these areas are characterized by the highest BVOC emitters (Appendix 1). This finding provides insights into the need for urban forestry policies that strategically select tree species with high pollutant removal capacity and low BVOC emissions to maximize air quality benefits while minimizing the risk of secondary pollution formation. It also suggests the importance of integrating GI design and zoning to reduce localized air quality challenges.

We found that the majority of the total BVOC emissions were observed in the stratum INS, while RES also exhibited elevated emissions. The spatial variability in BVOC emissions depends on land use type and specific tree species within a certain location. Urban parks in Hawassa exhibit the highest potential for O_3 and other secondary pollutants formation, with BVOC emissions predominantly concentrated within these GI types. Our observations highlight that *F. sur*, a native species known for its deciduous broadleaved and high-leaf area, is predominant in the two designated conservation parks, private resorts, and other forest patches. The two urban parks, locally named Gudmale and Millennium, are located at opposite ends of the city and feature native and introduced tree species with higher emission values (Fig. 8; Appendix 1). Likewise, overaged Eucalyptus plantation compartments, commonly found in these parks, were identified as the highest emitters. However, POVA and GB had higher average BVOC emission rates, despite having lower TCC and LAI. In terms of average emission, a prominent finding was that BVOC emissions were more pronounced in areas with lower TCC and higher temperatures, specifically in the less urbanized parts of Hawassa. This observation is consistent with Nowak et al. (2008), who reported that increased tree transpiration cools the air and reduces leaf temperatures, leading to decreased BVOC emissions. These effects are included in the Ecov6.0 model to account for how tree-induced cooling influences BVOC emissions during the growing season. These findings underscore the importance of urban design in managing BVOC emissions, which can inform more effective environmental policies and comprehensive urban planning strategies.

The role of urban trees in shaping air quality is multifaceted, depending on the configuration of GI, and can lead to both positive and negative effects on the environment. On the positive side, reduced wind speeds caused by GIs can lower heating energy use in buildings by minimizing cold air infiltration, which may lead to a reduction in pollutant emissions from power plants (Nowak, 2020b). Moreover, urban trees reduce wind speed, which helps to limit the mixing of polluted ground-level air with less contaminated upper air. This phenomenon leads to a concentration of pollutants in the lower layers, where pollution sources (e.g., parked vehicles in unventilated parking lots) are located. Therefore, careful design and configuration of GI systems are essential to balance these air quality impacts effectively. However, the benefits of GI on air quality enhancement should be evaluated against potential drawbacks. For example, reduced wind speeds can contribute to pollutant accumulation at ground level, potentially offsetting some benefits of cleaner upper air. Additional studies are required to assess these trade-offs in various built-up areas in Ethiopia, considering different GI configurations and seasonal variations.

This study did not address all contribution aspects of the GI system to urban air quality dynamics, as the Eco v6.0 model is limited in the context of Ethiopia to only quantify the dry deposition of air pollution through leaves. Although the model primarily estimates pollution removal through tree leaves, it does not account for other tree parts, such as bark, nor does it consider the role of urban trees in reducing pollution emissions from buildings in Ethiopia via cooling effects. This limitation arises because the model was originally developed based on U.S. building types, and customizing it to the Ethiopian context proved to be challenging (i-Tree Eco, 2020b). Despite this, the study confirmed that the model can be reliably used, with caution, to assess the environmental benefits of GI in African urban centers. Although this tool is less common in Africa, previous studies by Koricho et al. (2021) and Gebreyesus et al. (2023) have shown that careful adaptation in Ethiopian cities like Adama and Hawassa could yield meaningful result. Therefore, this study not only offers valuable insights for a specific location but also highlights the broader relevance of the innovative methods we employed for GI planning across Sub-Saharan Africa.

The i-Tree Eco v6.0 model introduces some uncertainties in our study, primarily related to unidentified estimation errors in calculating key variables such as leaf area, leaf biomass, and tree biomass. Additionally, while the model provides general air pollution removal values for shrubs, it lacks species-specific data, which may affect the accuracy of removal estimates. The model also simplifies complex physical and chemical interactions between trees and the atmosphere, such as local wind patterns and turbulence, both of which can impact pollutant removal and dispersion rates (i-Tree Eco, 2020c). Furthermore, the valuation of air purification benefits is based on the model's default economic values rather than localized data, potentially leading to discrepancies in the monetary assessment of these ecosystem services. Similarly, pollution estimates depend on concentration data from a single or an average of several monitors, limiting the spatial resolution (Nowak, 2020b). Despite these uncertainties, i-Tree Eco v6.0 is widely recognized and validated for assessing urban forest ecosystem services. We have accounted for these limitations in our analysis, and future research could improve accuracy by incorporating local data and refining assumptions specific to urban centers in Ethiopia.

5. Policy Implications

Despite the efforts of the government to promote greenery through strategies in Ethiopia, gaps remain between policy intentions and their implementation. The National Environmental Policy, established over two decades ago, and recent initiatives known as the National GI Implementation Standard emphasize the importance of green spaces (Girma et al., 2019). However, the reality on the ground often falls short of these goals, as the policies remain largely unimplemented (Flanagan et al., 2021). The national GI Standard recommends dedicating at least 30% of urban land to GI development (MUDH, 2015). However, no city has achieved this target, highlighting a critical gap between policy directives and tangible outcomes. Effective integration of GI requires the commitment of planners and policymakers to execute these GI standards and mainstream them into urban planning processes.

In Ethiopia, urban greenery is often seen primarily as an employment sector for university graduates and others without professional backgrounds, regardless of their prior skills in GI planning. This practice may lead to the wrong GI planning, increasing BVOC emissions, and ending up with less efficient GIs in improving air quality. For example, *G. robusta*, the dominant tree species in Hawassa, is the preferred species for planting in most urban centers of the country due to its rapid growth. Despite being one of the leading contributors to air pollution removal, this species is also one of the top monoterpenes emitters. This implies that a certain tree species with the highest BVOC emission nature does not mean it contributes less to removing pollution. Similarly, *C. megalocarpus*, an exotic deciduous species, was identified in this study as one of the BVOC emitters but is commonly planted along roadsides and street medians in Hawassa. Moreover, land tenure also poses a significant obstacle to the urban tree canopy increment in the study area. Urban land is often allocated arbitrarily for greenery, even if not designated as such in master plans, and these green spaces may be converted into other land uses without prior consultation. To maintain and expand tree cover amidst these challenges, one effective strategy could be converting vacant areas into green spaces. In this study, we identified a total of 2064 ha of urban land, representing approximately 40% of the total area of the city, as plantable land spaces. These "plantable spaces" should be unrestricted lands with suitable soil for tree growth, located away from structures and large trees to ensure new tree growth (i-Tree Eco, 2020a). Most of these spaces (35.7%) were found in residential areas, where the current tree coverage is only 18.9%, and converting these vacant areas could potentially double the city's current tree canopy coverage of 20.7%.

6. Conclusions and Recommendations

Systematically simulating how urban nature can address the environmental effects of urbanization provides a clearer understanding of its potential impact. This study emphasized on the substantial potential of GIs to enhance air quality while also drawing attention to the possible negative effects of GI systems that have been installed without proper care. The existing GIs in Hawassa contributed to 20.7% of tree cover and removed 274.2 t air pollution. While this pollution removal is substantial, the removal or emission of pollutants can change atmospheric systems, either positively or negatively. However, it is important to note that GI elements can adversely affect the environment due to the BVOC emission from some urban trees, which can contribute to the formation of pollutants. This dual role of urban trees necessitates a strategic approach to GI management in Ethiopia. Improving the ES offered by the existing GI in Hawassa and other urban centers in Ethiopia can be achieved by adopting proven strategies to enhance air quality, taking the unique location into account. GI integration and air quality emphasize the interconnected nature of GI and air quality issues and advocate for an integrated framework that aligns GI planning with air quality management. Thus, GIs should be integrated into spatial planning at the national level taking into account the 1) multi-functionality design: GI planning should deliver multiple benefits, including air quality improvement; 2) GI planners should carefully consider the location of high-BVOC-emitting species, ensuring they are planted in areas where their emissions will have less impact on secondary pollutant formation (e.g., away from high-traffic or industrial areas); 3) seasonal and spatial variability considerations: incorporating urban trees considering their air quality improvement roles accorded with the change of season and maximize their efficiency with proper configuration based on the land use types; 4) policy integration: urban planning policies should incorporate GI strategies as a pillar element to enhance air quality; and 5) economic valuation: residents and authorities should recognize that the ES provided from the well-planned GI can be converted into money comparable to income from selling land. However, further research is also needed to compare the quantified economic values of GI derived from ES (intangible benefits) and the monetary value gained from selling the same land (tangible benefits) where the GI elements have been constructed.

CRediT authorship contribution statement

Tikabo Gebreyesus: Writing – review & editing, Writing – original draft, Software, Project administration, Methodology, Investigation, Formal analysis, Data curation, Conceptualization. **Christian Borgemeister:** Writing – review & editing, Visualization, Validation, Supervision. **Cristina Herrero- Jáuregui:** Writing – review & editing, Visualization, Validation, Supervision. **Girma Kelboro:** Writing – review & editing, Visualization.

Declaration of competing interest

The authors declare that they have no known competing financial interests or personal relationships that could have appeared to influence the work reported in this paper.

Acknowledgment

We gratefully acknowledge the support of the **Paths to Research Program** at the University of Bonn for providing a scholarship to the corresponding author during his PhD studies.

Appendix A. Supplementary data

Supplementary data to this article can be found online at https://doi.org/10.1016/j.envpol.2024.125244.

Data availability

Data will be made available on request.

References

Amare, A.N., Sorsa, S., Gebremariam, Z., De Coster, G., Van Langenhove, H., Demeestere, K., Walgraeve, C., 2023. Volatile organic compounds in school environments of Hawassa city, Ethiopia and assessment of possible human health risks. Atmos. Pollut. Res. 14 (12). https://doi.org/10.1016/j.apr.2023.101943.

Amegah, A.K., Agyei-Mensah, S., 2017. Urban air pollution in sub-saharan Africa: time for action. Environmental Pollution 220, 738–743. https://doi.org/10.1016/j.envpol.2016.09.042. Elsevier Ltd.

Anderson, B., Patiño Quinchia, J.E., Prieto Curiel, R., 2022. Boosting African cities' resilience to climate change: the role of green spaces. In: West African Papers, No. 37. OECD Publishing, Paris. https://doi.org/10.1787/3303cfb3-en.

Baldocchi, D.D., Hicks, B.R.B., Mara, P., 1987. A canopy stomatal resistance model for gaseous deposition to vegetated surfaces. Atmos. Environ. 21 (167), 91–101.

Baró, F., Chaparro, L., Gómez-Baggethun, E., Langemeyer, J., Nowak, D.J., Terradas, J., 2014. Contribution of ecosystem services to air quality and climate change mitigation policies: the case of urban forests in Barcelona, Spain. Ambio 43 (4), 466–479. https://doi.org/10.1007/s13280-014-0507-x.

Baumgardner, D., Varela, S., Escobedo, F.J., Chacalo, A., Ochoa, C., 2012. The role of a peri-urban forest on air quality improvement in the Mexico City megalopolis. Environmental Pollution 163, 174–183. https://doi.org/10.1016/j.envpol.2011.12.016.

Bekele-Tesemma, A., 2007. Useful Trees of Ethiopia: Identification, Propagation, and Management in 17 Agroecological Zones. Nairobi: RELMA in ICRAF Project, 552p. RELMA in ICRAF Project, World Agroforestry Centre, Eastern Africa Region.

Benjamin, M.T., Winert, A.M., 1998. Estimating the ozone-forming potential of urban trees and shrubs. Atmos. Environ. 32 (I), 53.

Bottalico, F., Chirici, G., Giannetti, F., Marco, A. De, Nocentini, S., Paoletti, E., Salbitano, F., Sanesi, G., Travaglini, D., 2016. Air Pollution Removal by Green Infrastructures and Urban Forests in the City of Florence, vol. 8, pp. 243–251. https://doi.org/10.1016/j.aaspro.2016.02.099.

Calfapietra, C., Fares, S., Manes, F., Morani, A., Sgrigna, G., Loreto, F., 2013. Role of Biogenic Volatile Organic Compounds (BVOC) emitted by urban trees on ozone concentration in cities: a review. Environmental Pollution 183, 71–80. https://doi.org/10.1016/j.envpol.2013.03.012.

Chaparro, L., Terradas, J., 2009. Report on Ecological Services of Urban Forest in Barcelona. Department of Environment, Barcelona, Spain, p. 96. Barcelona City Council. www.creaf.uab.cat.

Cordell, R.L., Panchal, R., Bernard, E., Gatari, M., Waiguru, E., Ng'ang'a, M., Nyang'aya, J., Ogot, M., Wilde, M.J., Wyche, K.P., Abayomi, A.A., Alani, R., Monks, P.S., Vande Hey, J.D., 2021. Volatile organic compound composition of urban air in Nairobi, Kenya and Lagos, Nigeria. Atmosphere 12 (10). https://doi.org/10.3390/atmos12101329.

European Union, 2013. Building Green Infrastructure for Europe. European Commission, Luxembourg. https://doi.org/10.2779/54125.

Fairbrass, A., Jones, K., Mcintosh, A., Yao, Z., Malki-Epshtein, L., Bell, S., 2018. Green Infrastructure for London: A Review of the Evidence. Engineering Exchange for Just Space and the London Sustainability Exchange.

Federal Urban Planning Institute, 2006. *Integrated Development Plan Report for Hawassa City*. Ethiopia's Ministry of Works and Urban Development. Federal Urban Planning Institute (FUPI), Addis Ababa, Ethiopia.

Fetene, A., Worku, H., 2013. Planning for the conservation and sustainable use of urban forestry in Addis Ababa, Ethiopia. Urban For. Urban Green. 12 (3), 367–379. https://doi.org/10.1016/j.ufug.2013.03.004.

Flanagan, E., Mattisson, K., Walles, J., Abera, A., Eriksson, A., Balidemaj, F., Oudin, A., Isaxon, C., Malmqvist, E., 2021. Air pollution and urban green space: evidence of environmental injustice in Adama, Ethiopia. Frontiers in Sustainable Cities 3. https://doi.org/10.3389/frsc.2021.728384.

Gebreyesus, T., Yeshitela, K., Fetene, A., Jauregui, C.H., 2022. Study on the land surface cover dynamics of built - up areas and its implication for sustainable urban planning in Hawassa city , Ethiopia. Geojournal. https://doi.org/10.1007/s10708-022-10729-x, 0123456789.

Gebreyesus, T., Herrero, C., Kumelachew, J., Aramde, Y., Mesele, F., 2023. Rethinking urban planning from the perspective of nature - based stormwater runoff management in Ethiopia. Landsc. Ecol. Eng. https://doi.org/10.1007/s11355-023-00565-7, 0123456789.

Girma, Y., Terefe, H., Pauleit, S., 2019. Urban green spaces use and management in rapidly urbanizing countries:-The case of emerging towns of Oromia special zone surrounding Finfinne, Ethiopia. Urban For. Urban Green. 43 (April), 126357. https://doi.org/10.1016/j.ufug.2019.05.019.

Gong, C., Xian, C., Ouyang, Z., 2022. Assessment of NO2 purification by urban forests based on the i-tree Eco model: case study in Beijing, China. Forests 13 (3). https://doi.org/10.3390/f13030369.

Hawassa City Administration, 2017. Socio-economic Profile of Hawassa. Finance & Economic Development Department, Socio-Economic and Geo-Spatial Data Analysis & Dissemination Core Work Process, Hawassa, Ethiopia.

Hewitt, C.N., Ashworth, K., MacKenzie, A.R., 2020. Using green infrastructure to improve urban air quality (GI4AQ). Ambio 49 (1), 62–73. https://doi.org/10.1007/s13280-019-01164-3.

Hirabayashi, S., Kroll, C.N., Nowak, D.J., 2012. Development of a distributed air pollutant dry deposition modeling framework. Environmental Pollution 171, 9–17. https://doi.org/10.1016/j.envpol.2012.07.002.

Hirabayashi, S., Kroll, C.N., Nowak, D.J., 2015. I-Tree Eco Dry Deposition Model Descriptions.

i-Tree Database, 2020b. i-Tree tool. U.S. Forest Service. Retrieved from. https://www.itreetools.org/database.

i-Tree Eco, 2020a. I-Tree. I-Tree Eco User Manual. V6. the United States Department of Agriculture and Forest Service. https://www.itreetools.org/documents/134/i-Tree_Eco_Manual_v6.pdf.

i-Tree Ecov6, 2020b. I-Tree Eco User's Field Guide, 6.0. United State Department of Agriculture. Forest Services. https://www.itreetools.org/support/resources-overview/i-tree-manuals-workbooks.

i-Tree Eco, 2020c. I-Tree Eco Guide To International Projects. U.S. Forest Service, Washington, D.C., United States. *Retrieved from*. https://www.itreetools.org/tools/i-tree-eco.

Isaifan, R.J., Baldauf, R.W., 2020. Estimating economic and environmental benefits of urban trees in desert regions. Frontiers in Ecology and Evolution 8. https://doi.org/10.3389/fevo.2020.00016.

Jayasooriya, V.M., Ng, A.W.M., Muthukumaran, S., Perera, B.J.C., 2017. Green infrastructure practices for the improvement of urban air quality. Urban For. Urban Green. 21, 34–47. https://doi.org/10.1016/j.ufug.2016.11.007.

Kasim, O.F., Abshare, M.W., Mukuna, T.E., Wahab, B., 2018. Land use and ambient air quality in Bahir Dar and Hawassa, Ethiopia. Air Soil. Water Res. 11. https://doi.org/10.1177/1178622117752138.

Kim, K.G., 2018. Planning Models for Climate Resilient and Low-Carbon Smart Cities : an Urban Innovation for Sustainability , Ef Fi Ciency , Circularity , Resiliency , and Connectivity Planning, pp. 77–85. https://doi.org/10.1007/978-3-319-59618-1.

Koricho, H.H., Seboka, A.D., Fufa, F., Gebreyesus, T., Song, S., 2021. Study on the ecosystem services of urban forests: implications for climate change mitigation in the case of Adama City of Oromiya Regional Sate, Ethiopia. Urban Ecosyst. https://doi.org/10.1007/s11252-021-01152-0, 0123456789.

Kumar, P., Druckman, A., Gallagher, J., Gatersleben, B., Allison, S., Eisenman, T.S., Hoang, U., Hama, S., Tiwari, A., Sharma, A., Abhijith, K.V., Adlakha, D., McNabola, A., Astell-Burt, T., Feng, X., Skeldon, A.C., de Lusignan, S., Morawska, L., 2019. The nexus between air pollution, green infrastructure and human health. Environ. Int. 133. Elsevier Ltd. https://doi.org/10.1016/j.envint.2019.105181.

Lindley, S.J., Gill, S.E., Cavan, G., Yeshitela, K., Nebebe, A., Woldegerima, T., Kibassa, D., Shemdoe, R., Renner, F., Buchta, K., Abo-el-wafa, H., Printz, A., Oue, Y., Zogning, M. O.M., Tonye, E., 2015. Green infrastructure for climate adaptation in african cities. In: Pauleit, S., Coly, A., Fohlmeister, S., Gasparini, P., Jørgensen, G., Kabisch, S., Kombe, W.J., Lindley, S., Simonis, I., Yeshitela, K. (Eds.), Urban Vulnerability and Climate Change in Africa. Springer International Publishing Switzerland, pp. 153–196. https://doi.org/10.1007/978-3-319-03982-4.

McMichael, A.J., 2000. The urban environment and health in a world of increasing globalization: issues for developing countries. Bull. World Health Organ. 78 (Issue 9). https://doi.org/10.1590/S0042-96862000000900007.

Ministry of Urban Development and Housing (MUDH), 2015. Ethiopian National Urban Green Infrastructure Standards. Addis Ababa, Ethiopia.

Muresan, A.N., Sebastiani, A., Gaglio, M., Fano, E.A., Manes, F., 2022. Assessment of air pollutants removal by green infrastructure and urban and peri-urban forests management for a greening plan in the Municipality of Ferrara (Po river plain, Italy). Ecol. Indicat. 135. https://doi.org/10.1016/j.ecolind.2022.108554.

Nowak, D.J., 2020a. *Understanding I-Tree : Summary Of Programs And Methods* (Issue November). USDA Forest Service General. https://doi.org/10.2737/NRS-GTR-200. Technical Report N E- 1 86. Radnor.

Nowak, D.J., 2020b. Urban trees, air quality and human health. In: Christos, Gallis, Sop, Shin Won (Eds.), Forests for Public Health. Cambridge Scholars Publishing, Lady Stephenson Library, Newcastle upon Tyne, pp. 32–55. NE6 2PA, UK.

Nowak, D.J., Heisler, G.M., 2010. Air quality effects of urban trees and parks. National recreation and para k association, belmont ridge road ashburn, VA. Research Series Monograph 44. www.NRPA.org.

Nowak, D., Crane, D., 2000. The Urban Forest Effects (UFORE) Model: Quantifying urban forest structure and functions', in Integrated tools for natural resources inventories in the 21st century. Gen. Tech. Rep. NC-212, 714–720.

Nowak, D.J., Crane, D.E., Stevens, J.C., 2006. Air pollution removal by urban trees and shrubs in the United States. Urban For. Urban Green. 4 (3–4), 115–123. https://doi.org/10.1016/j.ufug.2006.01.007.

Nowak, D.J., Crane, D.E., Stevens, J.C., Hoehn, R.E., Walton, J.T., Bond, J., 2008. A ground-based method of assessing urban forest structure and ecosystem services. Arboric. Urban For. 34 (6), 347–358.

Nowak, D.J., Hirabayashi, S., Bodine, A., Greenfield, E., 2014a. Tree and forest effects on air quality and human health in the United States. Environmental Pollution 193, 119–129. https://doi.org/10.1016/j.envpol.2014.05.028.

Nowak, D.J., Hoehn, R.E., Crane, D.E., Stevens, J.C., Fisher, C.L., 2014b. Assessing Urban Forest Effects and Values: Douglas County, Kansas. U.S. Department of Agriculture, Forest Service, Northern Research Station. https://doi.org/10.2737/NRS-RB-91.

Nowak, B.D.J., Maco, S., Binkley, M., 2018a. I-tree : global tools to assess tree benefits and risks to improve forest management. ArboriculturAl ConsultAnt 51 (4), 10–13.

Nowak, D.J., Hirabayashi, S., Doyle, M., McGovern, M., Pasher, J., 2018b. Air pollution removal by urban forests in Canada and its effect on air quality and human health. Urban For. Urban Green. 29, 40–48. https://doi.org/10.1016/j.ufug.2017.10.019.

Ouyang, H., Tang, X., Kumar, R., Zhang, R., Brasseur, G., Churchill, B., Alam, M., Kan, H., Liao, H., Zhu, T., Chan, E.Y.Y., Sokhi, R., Yuan, J., Baklanov, A., Chen, J., Patdu, M. K., 2022. Toward better and healthier air quality implementation of WHO 2021 global air quality guidelines in asia. Bull. Am. Meteorol. Soc. 103 (7), E1696–E1703. https://doi.org/10.1175/BAMS-D-22-0040.1.

Parsa, V.A., Salehi, E., Yavari, A.R., van Bodegom, P.M., 2019. Analyzing temporal changes in urban forest structure and the effect on air quality improvement. Sustain. Cities Soc. 48. https://doi.org/10.1016/j.scs.2019.101548.

Rasoolzadeh, R., Mobarghaee Dinan, N., Esmaeilzadeh, H., Rashidi, Y., Sadeghi, S. M.M., 2024. Assessment of air pollution removal by urban trees based on the i-Tree Eco Model: The case of Tehran, Iran. Integrated Environ. Assess. Manag. https://doi.org/10.1002/ieam.4990.

Scott, R., Ross, I., Hawkins, P.M., 2016. Fecal sludge management: diagnostics for service delivery in urban areas - report of FSM study in Hawassa, Ethiopia (English). In: Water and Sanitation Program (WSP), Water and Sanitation Program Technical Paper. World Bank Group. Finance & Economic Development Department, Washington, D.C.

Selmi, W., Weber, C., Rivière, E., Blond, N., Mehdi, L., Nowak, D., 2016. Air pollution removal by trees in public green spaces in Strasbourg city, France. Urban For. Urban Green. 17 (2), 192–201. https://doi.org/10.1016/j.ufug.2016.04.010.

Song, P., Kim, G., Mayer, A., He, R., Tian, G., 2020. Assessing the ecosystem services of various types of urban green spaces based on i-Tree Eco. Sustainability 12 (4). https://doi.org/10.3390/su12041630.

Tessema, M.W., Abebe, B.G., Bantider, A., 2024. Physical and socio-economic driving forces of land use and land cover changes: the case of Hawassa City, Ethiopia. Front. Environ. Sci. 12. https://doi.org/10.3389/fenvs.2024.1203529.

United Nations Human Settlements Programme, 2022. World Cities Report 2022: Envisaging the future of cities. UN-Habitat. www.unhabitat.org.

Weather Spark, 2021. Climate and average weather year round in Hawassa, Ethiopia. Retrieved from. https://weatherspark.com/.

World Bank, 2017. Greening Africa's Cities: Enhancing the Relationship between Urbanization, Environmental Assets and Ecosystem Services. www.worldbank.org.

Xie, Y., Hirabayashi, S., Hashimoto, S., Shibata, S., Kang, J., 2023. Exploring the spatial pattern of urban forest ecosystem services based on i-tree Eco and spatial interpolation: a case study of kyoto city, Japan. Environ. Manag. 72 (5), 991–1005. https://doi.org/10.1007/s00267-023-01847-4.

Yang, J., Yu, Q., Gong, P., 2008. Quantifying air pollution removal by green roofs in Chicago. Atmos. Environ. 42 (31), 7266–7273. https://doi.org/10.1016/j.atmosenv.2008.07.003.

Yang, Y., Ma, J., Liu, H., Song, L., Cao, W., Ren, Y., 2023. Spatial Heterogeneity analysis of urban forest ecosystem services in Zhengzhou City. PLoS One 18 (6 June). https://doi.org/10.1371/journal.pone.0286800.

Yao, Y., Wang, Y., Ni, Z., Chen, S., Xia, B., 2022. Improving air quality in Guangzhou with urban green infrastructure planning: an i-Tree Eco model study. J. Clean. Prod. 369. https://doi.org/10.1016/j.jclepro.2022.133372.

Yona, Y., Matewos, T., Sime, G., 2024. Analysis of rainfall and temperature variabilities in Sidama regional state, Ethiopia. Heliyon 10 (7), e28184. https://doi.org/10.1016/j.heliyon.2024.e28184.